Title

Influence of injection-induced cooling on deviatoric stress and shear reactivation of preexisting fractures in Enhanced Geothermal Systems

Authors

Jeanne, Pierre

Rutqvist, Jonny

Dobson, Patrick F

Publication Date

2017-11-01

DOI

10.1016/j.geothermics.2017.08.003

Peer reviewed

Geothermics 70 (2017) 367–375

Contents lists available at ScienceDirect

Geothermics

journal homepage: www.elsevier.com/locate/geothermics

Influence of injection-induced cooling on deviatoric stress and shear reactivation of preexisting fractures in Enhanced Geothermal Systems

Pierre Jeanne*, Jonny Rutqvist, Patrick F. Dobson

Lawrence Berkeley National Laboratory, Energy Geosciences Division, Berkeley, CA 94720, USA

ARTICLE INFO

Keywords:
Geothermal reservoir
Injection
Thermal effect
Induced seismicity
Numerical simulation

ABSTRACT

Cold water injection into a hot, fractured, geothermal reservoir may trigger shear activation of pre-existing fractures that can help to enhance reservoir permeability, but may also result in unwanted seismicity. In this paper, we investigate through numerical modeling of a hypothetical geothermal reservoir how injection-induced cooling may influence the potential for shear activation, paying special attention to the evolution of deviatoric stress under various stress regimes. In each case, we consider either a reservoir with homogeneous hydraulic properties or the presence of a more permeable fracture zone intersecting the injection well. This fracture zone is either oriented in the maximum (S_{Hmax}) or minimum (S_{hmin}) horizontal stress direction. Our main finding is that depending on the configuration, injection-induced cooling stresses can favor or prevent shear reactivation of the preexisting fracture, and this effect can vary temporally and spatially.

1. Introduction

In the US, it is estimated that only 2% of the total geothermal energy stored between 3 and 10 km depth could be sufficient to provide the US primary energy for 2800 years (MIT, 2006). To exploit this huge geothermal resource the technology of extracting heat from an 'Enhanced Geothermal System' (EGS) is being developed. It consists of artificially enhancing or creating the permeability of the reservoir by hydraulic stimulation. Geothermal production is then carried out by cold water injected into the reservoir and hot water/steam recovery at production wells. This injection/extraction perturbs the in-situ stress state in the reservoir, potentially leading to the reactivation of preexisting fractures and/or possibly creating new fractures. These processes can be accompanied by microseismic events which could provide valuable information on the EGS development, but could also potentially result in felt seismic events that could be a nuisance to the local population. Therefore, it is important to understand the mechanisms that induce such microseismicity or seismic events because valuable information regarding the extent of a stimulation zone (Rutqvist et al., 2015), in situ stress field (Boyle and Zoback, 2013), fracture orientation (Verdon et al., 2011), fault zone location (Jeanne et al., 2014a), and on reservoir hydromechanical properties (Jeanne et al., 2014b) can be obtained by monitoring and analyzing these events.

It is well known that increased reservoir fluid pressure can bring faults closer to a state of failure and induce seismic events, whereas the role played by thermal effect on fracture stability is less well understood. The theory of thermoelasticity predicts that if the rock is subjected to both a temperature change and an applied stress state, then the resulting stress is the sum of the two (Jaeger et al., 2012, Eq. (1)).

$$\sigma_{xx} = 2G\varepsilon_{xx} + \lambda(\varepsilon_{xx} + \varepsilon_{yy} + \varepsilon_{zz}) + 3\alpha K\Delta T$$

$$\sigma_{yy} = 2G\varepsilon_{yy} + \lambda(\varepsilon_{xx} + \varepsilon_{yy} + \varepsilon_{zz}) + 3\alpha K\Delta T$$

$$\sigma_{zz} = 2G\varepsilon_{zz} + \lambda(\varepsilon_{xx} + \varepsilon_{yy} + \varepsilon_{zz}) + 3\alpha K\Delta T$$

$$\sigma_{xy} = 2G\varepsilon_{xy},\ \sigma_{xz} = 2G\varepsilon_{xz},\ \sigma_{xz} = 2G\varepsilon_{yz}. \quad (1)$$

with λ the Lame parameter, G the shear modulus, K the bulk modulus, ΔT the temperature variation, 3α the volumetric thermal expansion coefficient, ε the components of the strain tensor and σ the components of the stress tensor.

Eq. (1) shows that (i) thermally induced stresses are not caused by temperature changes *per se*, but rather by the combination of a change in temperature and a mechanical restraint that inhibits free expansion or contraction of the rock (Jaeger et al., 2012). This highlights the importance to consider a 3D thermal stress solution coupled to a 3D elastic stress analysis to study the fracture stability during geothermal operation. However, many studies about thermoelastic effect in geothermal systems consider either 1D (Elsworth, 1989; Nygren and Ghassemi, 2005) or 2D thermo-hydro-mechanical (THM) models (Kohl et al., 1995; de Simone et al., 2013; Izadi and Elsworth, 2013; Ghassemi and Tao, 2016) to investigate the influence of the thermo-poroelastic effects on a single fracture or a fracture zone. Some studies using a 3D

* Corresponding author.
E-mail address: pjeanne@lbl.gov (P. Jeanne).

http://dx.doi.org/10.1016/j.geothermics.2017.08.003
Received 15 March 2017; Received in revised form 23 June 2017; Accepted 2 August 2017
0375-6505/ Published by Elsevier Ltd.

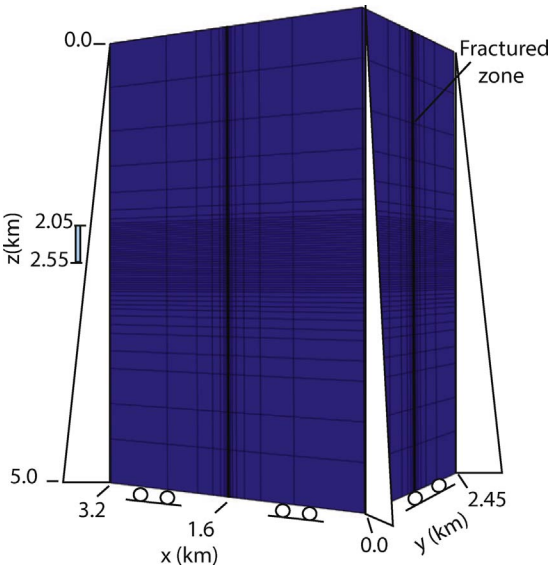

Fig. 1. Three dimensional numerical grids used to simulate a vertical injection well. The blue area along the z axis shows the position of the 500 m open section where injection occurs. (For interpretation of the references to colour in this figure legend, the reader is referred to the web version of this article.)

THM model were performed but with a 1D approach to model the temperature field and the thermal stress in the rock mass (Mossop, 2001; Kohl et al., 1995; Willis-Richards et al., 1996; Megel et al., 2005), and as reported by Ghassemi et al. (2003), a 1D heat transport model can underestimate the heat transfer from the rock to the fluid, and a 1D treatment of the elasticity problem does not predict the correct distribution of thermal stresses.

It is commonly believed that the temperature contrast between the injected cool water and the geothermal reservoir contributes to enhance the potential for induced seismicity. Thermal contraction of the rocks can reduce normal stresses and increase shear stresses on a fault promoting fault reactivation and induced seismicity (Ghassemi et al., 2007; Orlic et al., 2013). Thermal effects can also cause the rotation of the stress tensor below the cooling area promoting the observed long-term deepening of the microseismicity below active injection wells at The Geysers (California, US) as discussed by Jeanne et al. (2015a). The coupling between pore pressure and temperature also has a major role. The thermal contraction causes the fracture to open increasing the effective normal stress by reducing the pore pressure (Ghassemi and Tao, 2016). However, a recent study performed in support of the Northwest

Table 1
Hydraulic and mechanical properties.

	faulted reservoir		no fault
	reservoir	fault zone	reservoir
Young's modulus (GPA)	28	15	28
coefficient's Poison (−)	0.25	0.25	0.25
Biot coefficient (−)	1	1	1
Thermal conductivity (W/m°C)	3.2	3.2	3.2
Thermal expansion (°C $^{-1}$)	1.E-05	1.E-05	1.E-05
Specific heat (J/kg°C)	880	880	880
Permeability (m^2)	1.0E-15	1.0E-13	1.0E-13
Porosity (%)	5.0	15.0	15.0

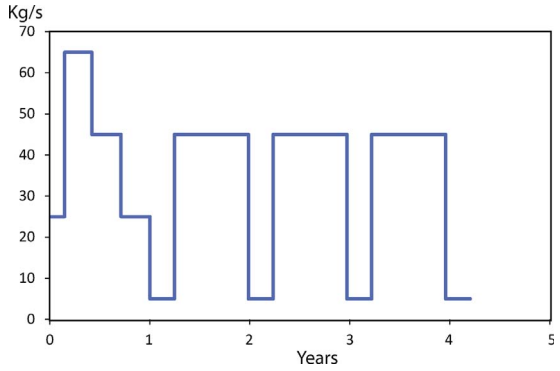

Fig. 3. Simulated injection rate.

Geysers EGS Demonstration Project(Jeanne et al., 2015b) suggests that thermal processes prevent shear reactivation and lead to the appearance of an aseismic domain just around the injection well. Jeanne et al. (2015b) explained this phenomenon by the fact that gravity-flow injected liquid into the host steam reservoir resulted in a preferential vertically extensive cooling zone that caused higher reduction in the vertical stress (S_V) than in the horizontal stresses. In the case of a normal stress regime this results in a decrease in deviatoric stress preventing shear reactivation of pre-existing fractures.

The motivation of this paper is to investigate the role of thermal processes on induced seismicity and to try to understand why thermo-mechanical effects can either favor or prevent shear reactivation of preexisting fractures. Here we investigate how the initial stress regime and the permeability tensor influences the induced-thermal stress variation and impact the induced seismicity. First we present the methodology, the numerical simulation used and our results.

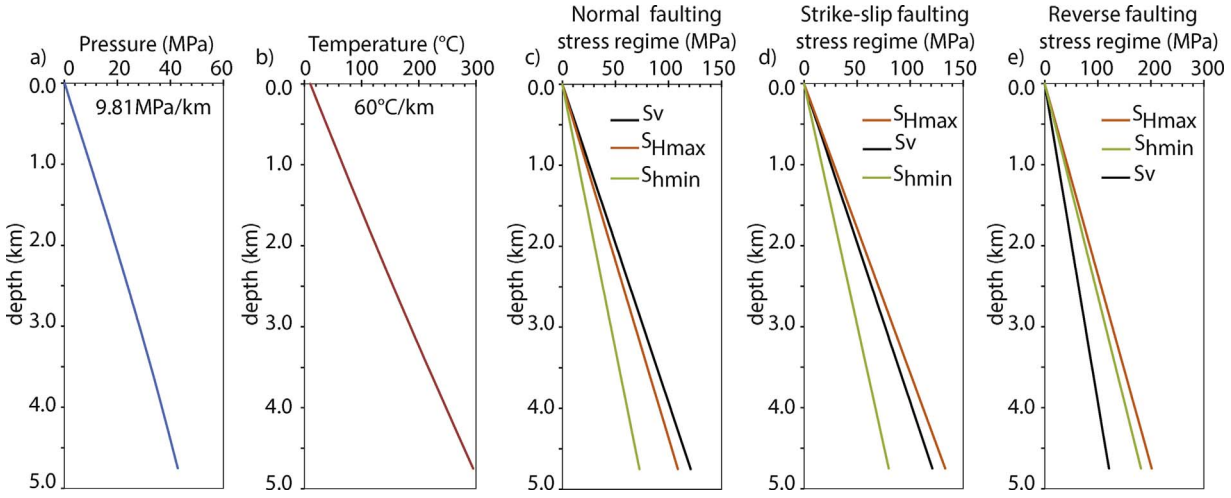

Fig. 2. (a) Hydraulic, (b) temperature and stress gradients used to simulate the (c) normal, (d) strike-slip and (e) reverse faulting regimes.

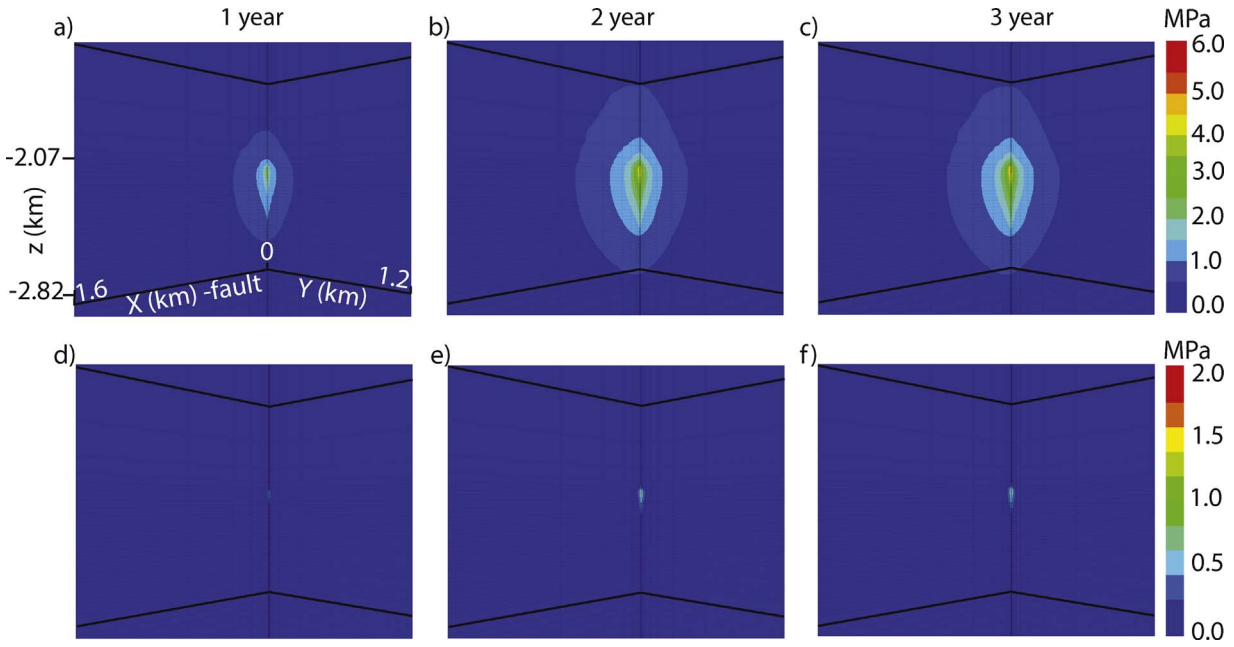

Fig. 4. Pressure distribution within (a–c) the fractured reservoir and (d–f) the reservoir with homogeneous hydraulic properties after 1, 2 and 3 years of injection.

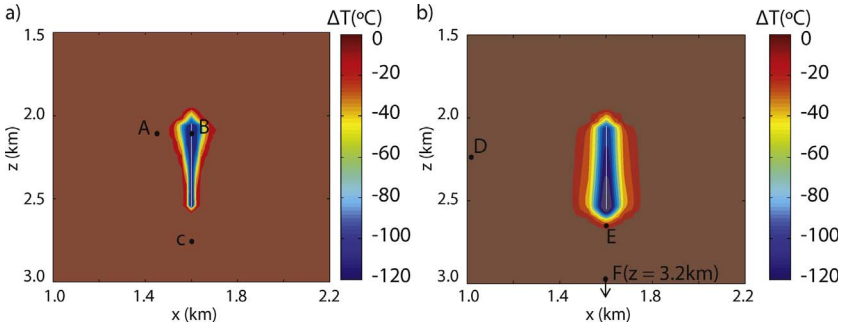

Fig. 5. Cross section along the fracture zone showing the changes in temperature after 260 days around the injection well (represented by a white line) in case of (a) a reservoir with homogeneous hydraulic properties and in case of (b) a fracture zone in the plane of the figure of high permeability intersecting the injection well.

2. Methodology

We simulate injection of cool water (40 °C) into a geothermal reservoir (≈130 °C at injection depth) subjected to a normal, strike-slip or reverse faulting stress regime. In each case, we consider either a reservoir with homogeneous hydraulic properties or the presence of a vertical fractured zone (6 m thick) intersecting the injection well on its entire length (500m) with a permeability two orders of magnitude higher than that of the host rock. This fracture zone is either oriented in the maximum (S_{Hmax}) or minimum (S_{hmin}) horizontal stress direction.

To study the induced thermal stresses, Thermo-Hydro-Mechanical (THM) and Hydro-Mechanical (HM) simulations are performed for each scenario and changes in stresses obtained during the HM simulation are subtracted from those obtained during the THM simulation. This approach allows for clearly identifying the role of Thermo-Mechanical (TM) effects and their influence on the deviatoric stress. In the following, changes in deviatoric stress caused by thermal effect are represented by changes in the Mohr circle radius: R_{tm} (Eq. (2)). An increase in R_{tm} brings the Mohr circle closer to the failure envelope and thus favors shear reactivation of a preexisting fracture, and inversely a decrease in R_{tm} tends to prevent shear reactivation:

$$R_{tm} = [(\sigma'_{1thm} - \sigma'_{1hm}) - (\sigma'_{3thm} - \sigma'_{3hm})]/2, \quad (2)$$

with $\sigma' = \sigma - Pf$, where Pf is the fluid pressure.

3. Model setup

We used the coupled THM simulator TOUGH-FLAC, described in Rutqvist et al. (2002) and Rutqvist (2011). TOUGH-FLAC links the TOUGH2 (finite volume) multiphase flow and heat transport simulator (Pruess et al., 2011) and the FLAC3D (finite-difference) geomechanical code (Itasca, 2009) for coupled THM analysis under multiphase flow conditions.

The numerical model domain is 3.2 × 2.45 × 5.0 km (Fig. 1) containing a vertical fracture zone of 6 m in thickness. The rock mass and the fracture zone behave as an elastic material. The pressure is hydrostatic, with a linear gradient of 9.81 MPa/km (Fig. 2a) and the temperature follows a geothermal gradient of 60 °C/km (Fig. 2b). Constant pressure is set on the boundaries to avoid any boundaries effects. The THM properties are listed in Table 1. The top boundary is free to move, whereas stresses on the other boundaries follow the lithostatic gradient. We simulate the cases of normal (Fig. 2c), strike-slip (Fig. 2d) and reverse faulting stress regimes (Fig. 2e). All of the simulations have the vertical stress defined as $S_v = \rho \times g \times z$, (with ρ the rock density, g the acceleration of gravity and z the depth), $\sigma_2 = \sigma_1 \times 0.9$ and $\sigma_3 = \sigma_1 \times 0.6$, with σ_1, σ_2 and σ_3 representing the maximum, the intermediate and the minimum principal stresses.

The simulated well in each case has a vertical 500 m long open-hole section where water is injected into the reservoir from 2050 m to 2550 m depth. First, we simulate an initial stimulation phase of 260 days where the injection takes place with steps of increasing and decreasing rates. Then, we simulate three years with seasonal variations

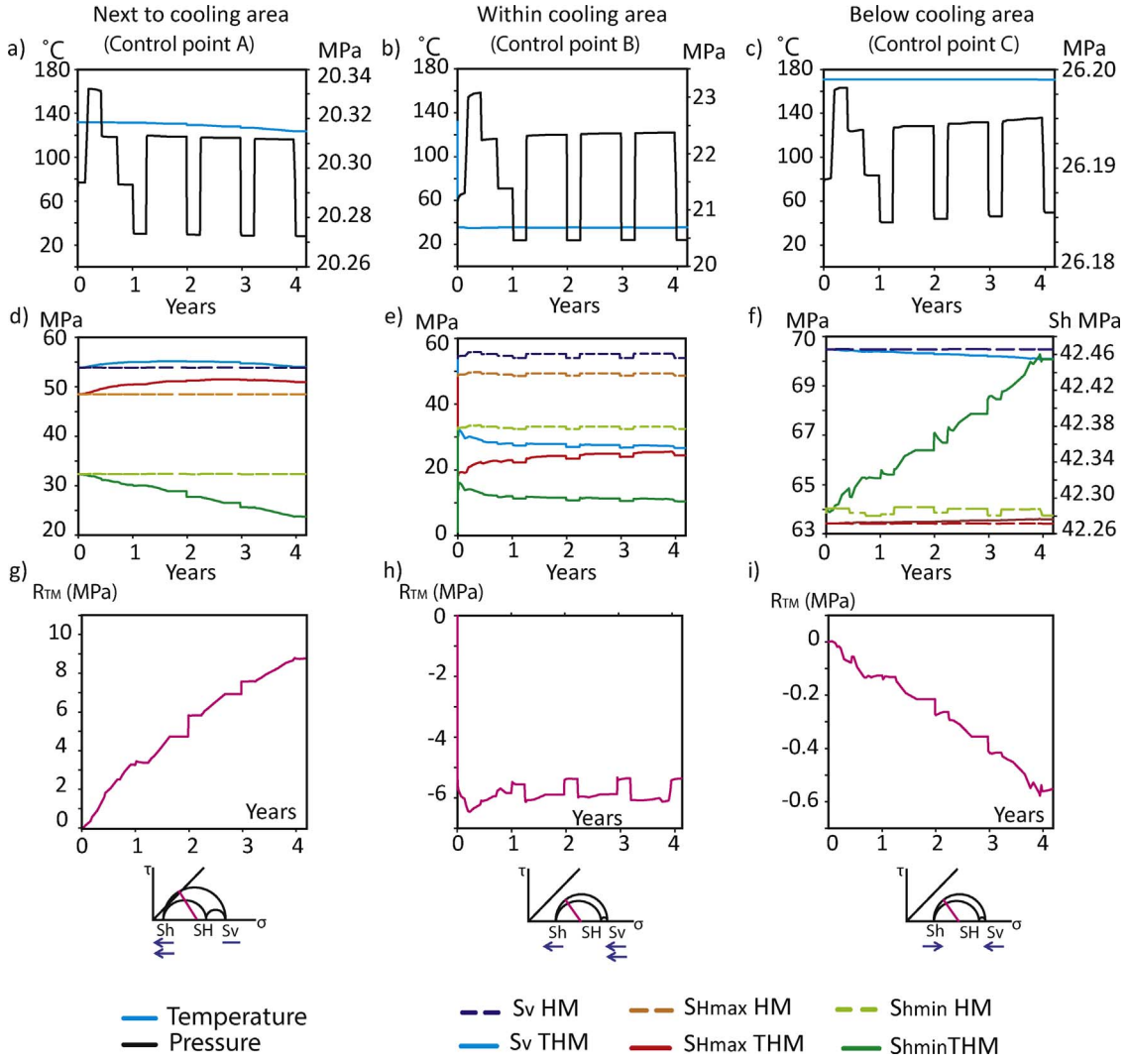

Fig. 6. Case of a vertical well within a reservoir with homogeneous hydraulic properties subjected to a normal stress regime. (a–c) Pressure and temperature history, (d–f) S_V, S_{Hmax} and S_{hmin} evolution during the HM and THM simulations and (g–i) changes in deviatoric stress due to TM effect (R_{tm} parameter) beside (control point A), within (control point B) and below (control point C) the cooling area.

in the injection rate (high rate during 9 months and low rate during 3 months) (Fig. 3). This injection pattern is used to investigate the influence of sharp pressure variations on the thermal effect.

4. Results

Fig. 4 shows the temporal and spatial changes in pressure after one, two and three years of injection in case of the fractured (Fig. 4a–c) and un-fractured reservoirs (Fig. 4d–f). Changes in pressure are more important into the fractured reservoir, because of the lower permeability of the host rock. Fig. 5 shows the changes in temperature at the end of the stimulation phase (260 days) around the vertical well in the case of a reservoir with homogeneous hydraulic properties (Fig. 5a) and in the case of a fracture zone of high permeability intersecting the well (Fig. 5b). We first present in detail how these changes in temperature influence S_V, S_{Hmax}, S_{hmin} and the deviatoric stresses in the case of a reservoir subjected to a normal stress regime with homogeneous hydraulic properties and with a fracture zone intersecting the injection well. The fracture zone is either oriented in the S_{Hmax} or S_{hmin} direction. Then, because thermally induced changes in S_V, S_{Hmax} and S_{hmin} are not influenced by the initial stress regime we only present in Section 4.3 changes in deviatoric stresses in case of strike-slip and reverse faulting regimes.

4.1. Case of a reservoir with homogeneous hydraulic properties and subjected to a normal stress regime

Fig. 6 shows the pressure, temperature and stress evolution over 4 years of injection at locations next to, within and below the vertical injection well (control points A–C in Fig. 5a) in the case of a reservoir with homogeneous hydraulic properties. The pressure evolution is more or less affected by the variations in the injection rate depending on the distance from the injection zone (Fig. 6a–c). The injection-induced cooling is a slower process apparently unaffected by the variation in injection rate. Changes in temperature are more persistent, which result either in a progressive decrease in temperature over the years around the injection zone or in a strong and constant decrease within the injection zone. Changes in temperature are small (≈ 9 °C) (Fig. 6a), high (≈ 100 °C) (Fig. 6b) or null (Fig. 6c) at the three control points located next to, within and below the injection well, respectively.

In the HM simulation, changes in stresses are small, up to: $\approx 3.0 \times 10^{-2}$ MPa (Fig. 6d), ≈ 2.0 MPa (Fig. 6e), and $\approx 1.0 \times 10^{-2}$ MPa (Fig. 6f), at these three control points during peak injection. The pressure changes are a result of a low injection rate and high permeability used in our simulations. Under these conditions, the poromechanical effects can only have a small influence on the stresses. In the THM simulation, changes in stresses are much larger and do not

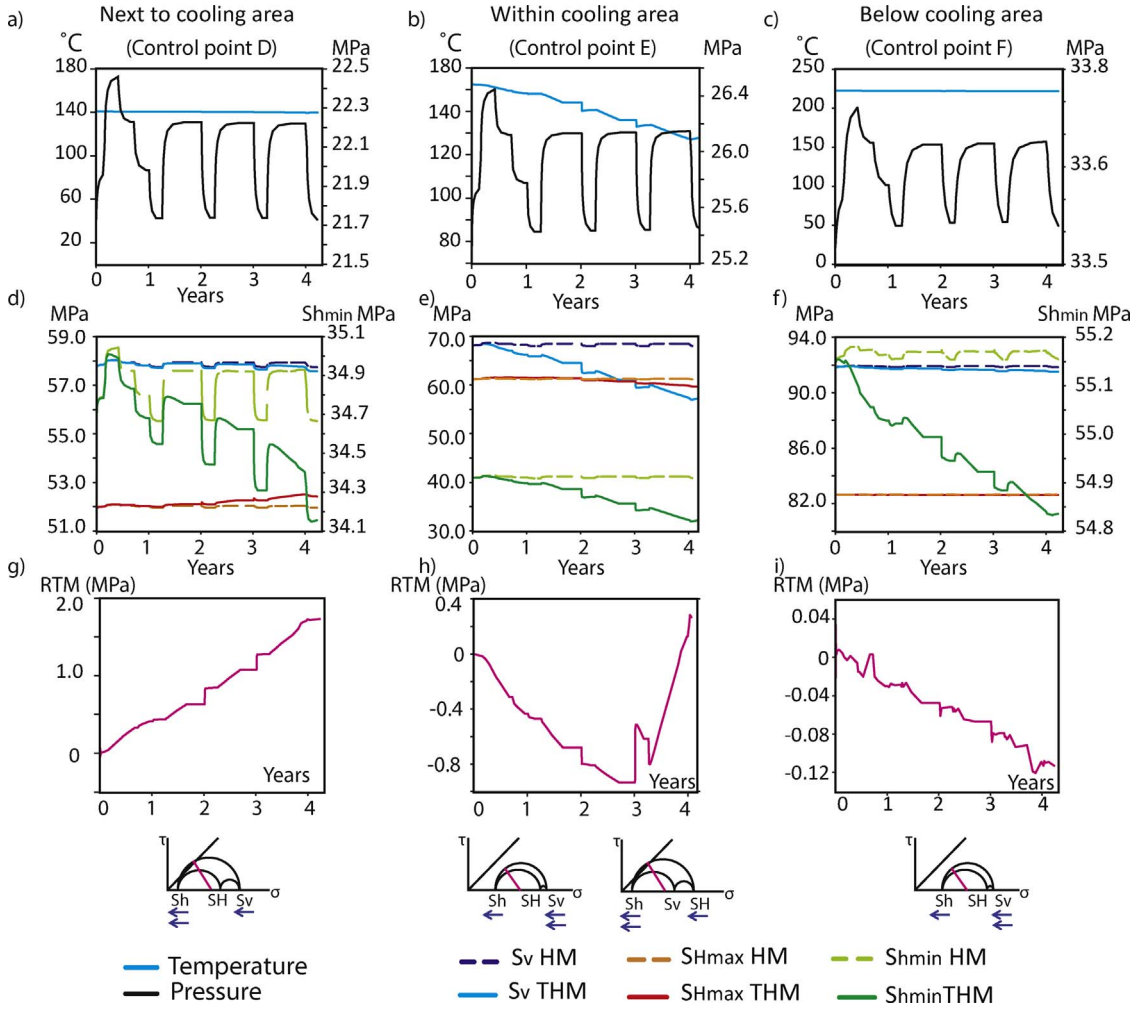

Fig. 7. Pressure and temperature evolution during the HM and THM simulations (a) next to, (b) within and (c) below the cooling area. Stress evolutions in the case of an initial normal stress faulting regime with a fracture zone parallel to S_{Hmax} during the HM and THM simulations, and the associated changes in the R_{tm} parameter (g and g) next to, (e and h) within and (f and i) below the cooling area.

follow the seasonal variation of the injection rate. For example, within the injection zone S_V and S_{hmin} decrease up to 27 MPa and 21 MPa, respectively (Fig. 6e). It also appears that, in the THM simulation, significant changes in stress occur in areas where few or no changes in temperature are calculated as in point A (Fig. 6a and d) and C (Fig. 6c and f), meaning that thermally induced strain and stress within the cooling area cause stress redistribution all around it. This stress redistribution leads to:

- next to the injection well: an increase in S_V and S_{Hmax} and a decrease in S_{hmin} (Fig. 6d),
- below the injection well: an increase in S_{hmin} and S_{Hmax} and a decrease in S_V (Fig. 6f).

These stress changes result in a decrease in deviatoric stress within and below the cooling area (Fig. 6h and i) and an increase next to the cooling area (Fig. 6g).

4.2. Case of injection into a fracture zone subjected to a normal stress regime

We investigate the cases where the injection well is intersected by a permeable fracture zone oriented either parallel (Fig. 7) or perpendicular (Fig. 8) to S_{Hmax} direction in case of a normal stress regime. Fig. 7 and 8 show the pressure, temperature and stress evolutions over 4 years of injection at locations next to, within and below the vertical injection well (control points D, E and F in Fig. 5b). For both fracture zone orientations, the pressure evolution is strongly affected by the variations in the injection rate (Fig. 7a–c), whereas within the cooling area changes in temperature progressively decrease over time (Fig. 7b). Also, because of the low injection rate and the high permeability the induced pressure changes are small (only 1 MPa) and so the poromechanical effects have very little impact on the stresses (less than 1 MPa). We only observe a slight increase in S_V, S_{Hmax} and S_{hmin} during peak injection.

In the THM simulation changes in stresses are greater. Within the cooling area (control point E), S_V strongly decreases for both fracture zone orientations, whereas changes in the horizontal stresses depend on the fracture zone orientation and associated horizontal fluid flow direction. When the injected cool water flows along the fracture:

- in S_{Hmax} direction: S_V and S_{hmin} decrease and S_{Hmax} stays almost constant (Fig. 7e),
- in S_{hmin} direction: S_V and S_{Hmax} decreases and S_{hmin} stays constant (Fig. 8b).

These two responses influence the deviatoric stress differently (Figs. 7 h and 8 e). Globally, it can be observed that S_V (here equal to the maximum principal stress σ_1) decreases more than S_{hmin} or S_{Hmax}, and so the R_{TM} parameter decreases. In the case of a fracture zone parallel to S_{Hmax}, after 3 years of injection S_V becomes lower than S_{Hmax} (Fig. 7e)

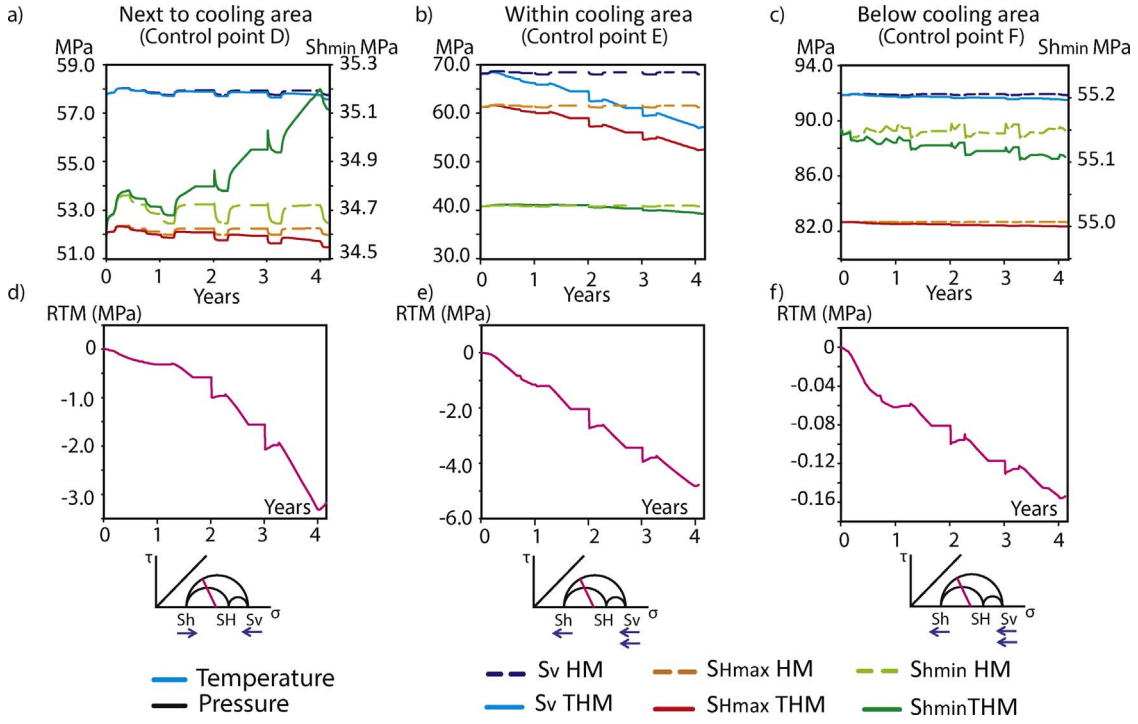

Fig. 8. Stress evolutions in the case of an initial normal stress faulting regime with a fracture zone perpendicular to S_{Hmax} during the HM and THM simulations, and the associated changes in the R_{tm} parameter (a and d) next to, (b and e) within and (c and f) below the cooling area.

and within the cooling area the in situ state of stress becomes a strike-slip faulting regime. Under this stress regime, S_V and S_{hmin} keep decreasing while S_{Hmax} (now equal to σ_1) stays constant leading to an increase in the R_{TM} parameter (Fig. 7h).

These thermally induced stresses causes stress redistribution around the cooling area (control points D and F). When the injected cool water flows:

- in S_{Hmax} direction:
  - Next to the cooling area (control point D): S_{hmin} decreases more than Sv and S_{Hmax} increases (Fig. 7d) leading to an increase in the R_{TM} parameter (Fig. 7g).
  - Below the cooling area (control point F): Sv decreases more than S_{hmin} and S_{Hmax} stays constant (Fig. 7f). The R_{TM} parameter decreases (Fig. 7i).
- in S_{hmin} direction:
  - Next to the cooling area (control point D): S_{hmin} increases whereas Sv and S_{Hmax} decrease (Fig. 8a). The R_{TM} parameter decreases (Fig. 8d).
  - Below the cooling area (control point F): Sv decreases more than S_{hmin} and S_{Hmax} (Fig. 8c). The R_{TM} parameter decreases (Fig. 8f).

These different effects could potentially favor and prevent shear slip along pre-existing fractures, as illustrated in Figs. 7 and 8 by several schematic Mohr-circles.

4.3. Cases of a reservoir with or without fracture zone subjected to a strike-slip or reverse stress regime

To gain insight on how the relation between the fluid flow direction and the *in-situ* stress can influence the changes in deviatoric stress caused by the TM effect (R_{TM} parameter) and so influence the stability of preexisting fractures, several simulations were performed where the initial stress regime and the permeability tensor were changed. It was observed that the initial stress regime does not influence the thermally induced changes in S_V, S_{Hmax} and S_{hmin} described previously, however the deviatoric stress evolves differently depending on the initial stress regime.

Fig. 9 summarizes the evolution of the thermally induced changes in S_V, S_{Hmax} and S_{hmin} in case of an injection well intersected by a fracture zone oriented parallel to the (a) S_{Hmax} and (e) S_{hmin} direction and in case of a reservoir with (i) homogeneous properties. Then, for these three cases, the impacts of changes in S_V, S_{Hmax} and S_h on the R_{TM} parameter are presented for normal, strike-slip and reverse faulting regimes. Fig. 10 shows the distribution of the changes in the R_{tm} parameter at the end of the stimulation phase (260 days).

When the injected cool water flows in the S_{Hmax} direction (Fig. 9a–d), we observe that:

- In case of a normal faulting regime (Fig. 9b), there is a decrease in the R_{TM} parameter below and within the cooling area because of a greater drop in σ_1 (S_V) than in σ_3 (S_{hmin}). Next to the cooling area σ_3 (S_{hmin}) decreases more than σ_1 (S_V) and so the R_{TM} parameter increases.
- In the cases of strike-slip (Fig. 9c) and reverse faulting regimes (Fig. 9d), below and within the cooling area the drop in σ_3 (S_{hmin} or S_V) is greater than the drop in σ_1 (S_{Hmax}) and so the deviatoric stress increases. Next to the cooling area σ_3 (S_{hmin} or S_V) decreases whereas σ_1 (S_{Hmax}) increases which results in an increase in the R_{TM} parameter.

When the injected cool water flows in the S_{hmin} direction (Fig. 9e–h), we observe that:

- In the cases of normal (Fig. 9f) and strike-slip (Fig. 9g) faulting regimes, there is a general decrease in the R_{TM} parameter. Below and within the cooling area, the drop in σ_1 (S_v or S_{Hmax}) is higher than the drop in σ_3 (S_{hmin}) and next to the cooling area σ_3 (S_{hmin} or S_V) decreases whereas σ_1 (S_{Hmax}) increases.
- In case of a reverse faulting regime (Fig. 9h), there is an increase in the R_{TM} parameter below and within the cooling area, because the drop in σ_3 (S_v) is higher than the drop in σ_1 (S_{Hmax}). Next to the cooling area we observed the opposite with a decrease in the R_{TM} parameter caused by a higher drop in σ_1 (S_{Hmax}) than in σ_3 (S_v).

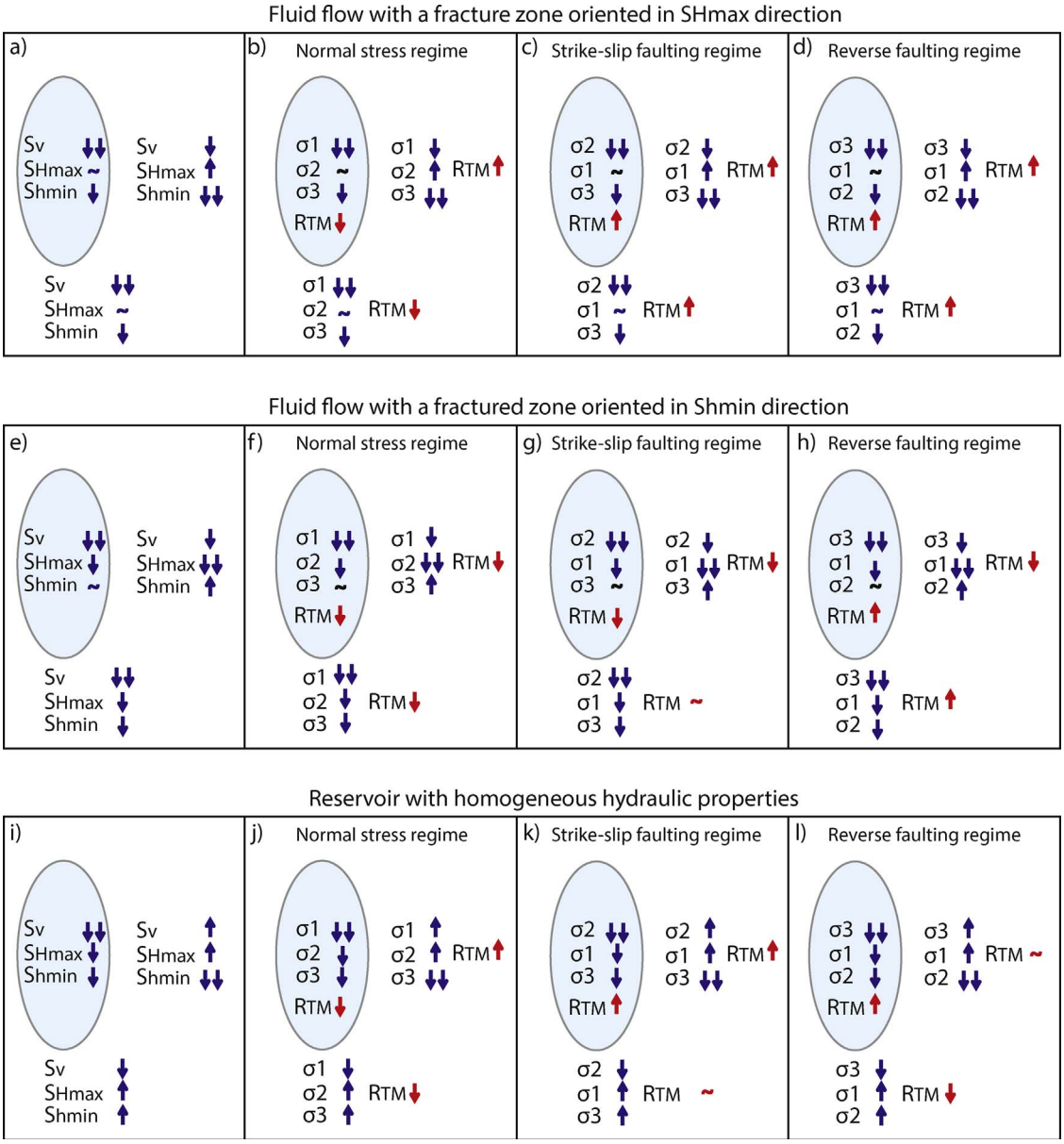

Fig. 9. Thermally induced changes in S_V, S_{Hmax} and S_{hmin} in the case of an injection well intersected by a fracture zone oriented in (a) S_{Hmax}, in (e) S_{hmin} direction and in case of a reservoir with (i) homogeneous properties and their impacts on the R_{TM} parameter in case of a (b–d) normal, (f–h), strike-slip and (j–l) reverse faulting regime.

In case of a reservoir with homogeneous hydraulic properties, we observe that:

- Within the cooling area, the drop in S_v is greater than the drop in horizontal stress. Therefore, the R_{TM} parameter will decrease a lot, a little or increase in the cases of normal, strike-slip and reverse faulting regimes, respectively.
- Next to the cooling area, the stress redistribution leads to an increase in S_V and S_{Hmax} increasing the R_{TM} parameter for the three stress regime.
- Below the cooling area, the stress redistribution leads to a decrease in S_V and an increase in S_{hmin} and S_{Hmax} resulting in a decrease in the R_{TM} parameter for the three stress regimes.

5. Discussions

5.1. Induced thermal stresses—general behavior

Our simulation results show that depending on (i) the fluid flow direction, (ii) the initial stress regime, (iii) the time and (iv) the location relative to the cooling area, induced thermal stresses can favor or prevent shear reactivation of preexisting fractures. The main factor controlling this process is the shape of the cooling area. As explained by Eq. (1) thermally induced stresses are caused by the combination of a change in temperature and a mechanical restraint that inhibits free expansion or contraction of the rock (Jaeger et al., 2012), and as suggested by Eq. (1) we show that the different components of the stress tensor could evolve differently for the same change in temperature. When fluid flows within a fracture zone the cooling area becomes penny shaped (as illustrated in Fig. 11a). In this case, the thermally induced stresses occurring within the penny edge (in the y direction in Fig. 11a) are restrained by the surrounding rock mass, which does not contract. Inversely, the thermally induced stresses occurring on the largest surface ("the penny's face") of the cooling area are less restrained by the surrounding rock, which is also contracting. For example in Fig. 11, a point on the largest surface of the cooling area at its center will easily deform in the x and z directions because all the surrounding rock also deforms in these two directions and so do not

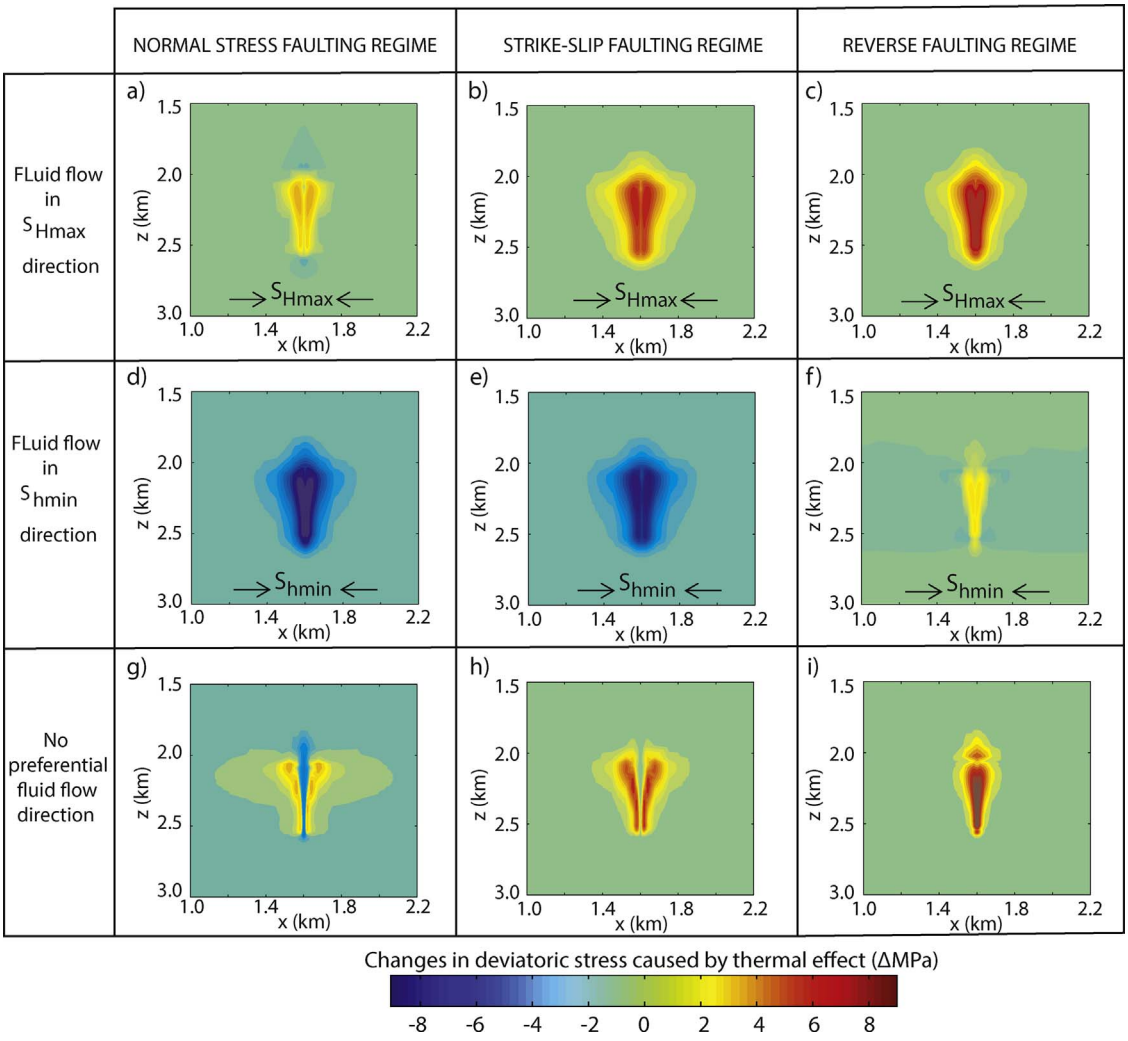

Fig. 10. Changes in deviatoric stress caused by thermal effect (represented by the R_{tm} parameter) at the end of the stimulation phase (260 days) in the case of a vertical well.

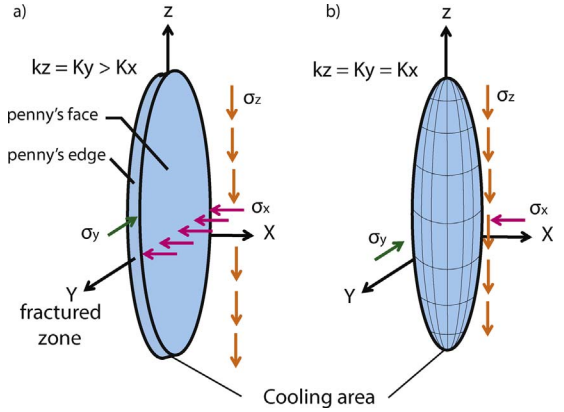

Fig. 11. Schematic view of the relation between the shape of the cooling area: (a) a penny shape and (b) a prolate spheroid and the stress acting on it in case.

restrain the deformations in these directions. The consequence is that the stresses acting on the largest surface of the cooling area ("the penny's face", see Fig. 11) are much more influenced by the thermal processes than the stress acting on the smallest surface of the cooling area ("the penny's edge", see Fig. 11) and this cause the vertical stress, the normal stress and the shear stress acting on the fracture zone to evolve differently for the same changes in temperature. In the same way, in case of a reservoir with homogeneous hydraulic properties, the cooling area extends laterally homogeneously and has a higher length in the vertical direction because of the gravity fluid flow (as illustrated in Fig. 11b). The horizontal mechanical restraint that inhibits the rock contraction will be very similar in S_{hmin} or in S_{Hmax}, whereas the vertical mechanical restraint will be much lower and the vertical and horizontal stresses will evolve differently.

5.2. Influence of the HM parameters on the TM effects

In our simulations, the hydraulic properties and the pore pressure were not affected by changes in temperature. Previous studies have shown that injection-induced cooling of the rock can results in fractures opening increasing their permeability (Bower and Zyvoloski, 1997), which can reduce the pore pressure within the cooling area and so favor the fluid diffusion. These THM effects were not analyzed here. Our goal was to investigate the TM effects on fracture stability on a long time scale (higher than the time scale for pore pressure diffusion). In this study, we show that the injection-induced cooling is a slow process poorly affected by the variation in injection rate and so in fluid pore pressure. This suggests that despite the absence of fully THM coupling in our simulations, the effects of injection-induced cooling on the fracture stability highlighted in this study should be observed during reservoir operation on a long time scale.

Also, we have considered only one single set of hypothetical hydraulic and mechanical parameters. Different parameters will influence the size of the cooling area and the amount of the induced-thermal

stress variation but not the general TM behavior observed and describe here. However, it should be noticed that we have considered only a geothermal reservoir with isotropic mechanical properties, and according to Eq. (1) a strong anisotropy in mechanical properties (as widely observed in metamorphic rock formation) may also strongly influence the distribution and the amount of induced-thermal stress.

5.3. Influence on the thermal stress on the shape and density of the induced-seismic cloud

Microseismic activity can provide valuable information on the EGS development so it is important to understand the causes and the mechanisms that induce microseismicity. Our study and especially Fig. 9 can be used to better understand the relation between the development of a cooling area and the distribution of the microseismicity. For examples in case of a geothermal system:

- With a normal faulting regime, within the cooling area thermal stress should prevent shear reactivation of the preexisting fracture. This phenomenon was discussed by Jeanne et al. (2015b) where they observed the appearance of an aseismic domain just around the injection well during EGS operation. In their paper, the growth of the seismically quiet domain around the injection matches the growth of the cooling area.
- Also for example, in case of a reverse faulting regime with a preferential fluid flow in S_{hmin} direction, the thermal stress will mostly favor rupture within and below the cooling area and not next to it. This can result in the development of a thin and elongated seismic cloud along the vertical axis. Whereas in other cases (strike-slip and reverse faulting regime with a preferential fluid flow in S_{Hmax} direction) thermal stress will favor rupture everywhere in the reservoir and so favor the development of a seismic cloud with a more spherical shape.

6. Conclusions

In this study, we investigate how the initial stress regime and the permeability tensor influence thermally induced stresses and deviatoric stresses. We simulated injection of cool water at low injection rates into a vertical well within a permeable geothermal reservoir subjected to different faulting stress regimes. We show that depending on (i) the fluid flow direction, (ii) the initial stress regime, (iii) the time and (iv) the location relative to the cooling area, induced thermal stresses can favor or prevent the reactivation of the preexisting fractures.

Acknowledgments

This work was supported by the U.S. Department of Energy, Office of Energy Efficiency and Renewable Energy, Geothermal Technologies Office under Contract No. DE-AC02-05CH11231 with Lawrence Berkeley National Laboratory.

References

Bower, K., Zyvoloski, G., 1997. A numerical model for thermo-hydro-mechanicalcoupling in fractured rock. Int. J. Rock Mech. Min Sci. 34 (8), 1201–1211.
de Simone, S., Vilarrasa, V., Carrera, J., Alcolea, A., Meier, P., 2013. Thermal coupling may control mechanical stability of geothermal reservoirs during cold water injection. J. Phys. Chem. Earth 64, 117–126.
Elsworth, D., 1989. Thermal permeability enhancement of blocky rocks: one-dimensional flows. Int. J. Rock Mech. Min. Sci. 26 (3–4), 329–339.
Ghassemi, A., Tao, Q., 2016. Thermo-poroelastic effects on reservoir seismicity and permeability change. Geothermics 63, 210–224.
Ghassemi, A., Tarasovs, S., Cheng, A.H.-D., 2003. An integral equation method for modeling three-dimensional heat extraction from a fracture in hot dry rock. Int. J. Numer. Anal. Methods Geomech. 27, 989–1004.
Ghassemi, A., Tarasovs, S., Cheng, A.H.-D., 2007. A three-dimensional study of theeffects of thermo-mechanical loads on fracture slip in enhanced geothermal reservoir. Int. J. Rock Mech. Min. Sci. Geomech. Abstr. 44, 1132–1148.
Itasca, 2009. FLAC3D, Fast Lagrangian Analysis of Continua in 3 Dimensions Version 4.0. Itasca Consulting Group, Minneapolis, Minnesota.
Izadi, G., Elsworth, D., 2013. The effects of thermal stress and fluid pressures on induced seismicity during stimulation to production within fractured reservoirs. Terra Nova 25, 374–380.
Jaeger, J.C., Cook, N.G.W., Zimmerman, R.W., 2017. Fundamentals of Rock Mechanics, 4th ed. Wiley-India editionpp. 475.
Jeanne, P., Rutqvist, J., Hartline, C., Garcia, J., Dobson, P.F., Walters, M., 2014a. Reservoir structure and properties from geomechanical modeling and microseismicity analyses associated with an Enhanced Geothermal System at The Geysers, California. Geothermics 51, 460–469.
Jeanne, P., Rutqvist, J., Vasco, D., Garcia, J., Dobson, P.F., Walters, M., Hartline, C., Borgia, A., 2014b. A 3D hydrogeological and geomechanical model of an enhanced geothermal system at The Geysers, California. Geothermics 51, 240–252.
Jeanne, P., Rutqvist, J., Dobson, P.F., Garcia, J., Walters, M., Hartline, C., Borgia, A., 2015a. Geomechanical simulation of the stress tensor rotation caused by injection of cold water in a deep geothermal reservoir. J. Geophys. Res. Solid Earth 120, 8422–8438.
Jeanne, P., Rutqvist, J., Rinaldi, A.P., Dobson, P.F., Walters, M., Hartline, C., Garcia, J., 2015b. Seismic and aseismic deformations and impact on reservoir permeability: the case of EGS stimulation at The Geysers, California, USA. J. Geophys. Res. Solid Earth 120. http://dx.doi.org/10.1002/2015JB012142.
Kohl, T., Evans, K.F., Hopkirk, R.J., Ryback, L., 1995. Coupled hydraulic, thermal, andmechanical considerations for the simulation of hot dry rock reservoirs. Geothermics 24, 345–359.
MIT, 2006. The Future of Geothermal Energy: Impact of Enhanced Geothermal Systems (EGS) on the United States in the 21 St Century. MIT Press.
Megel, T., Kohl, T., Rose, P., 2005. Reservoir modeling for stimulation planning at the Coso EGS project. Geotherm. Res. Council Trans. 29, 173–176.
Mossop, A., 2001. Seismicity, Subsidence and Strain at the Geysers GeothermalField. Ph.D. Dissertation. Stanford Universitypp. 51.
Nygren, A., Ghassemi, A., 2005. Influence of cold water injection on critically stressed fractures in Coso geothermal field, CA. In: Proceedings of the 39th US Rock Mechanics Symposium. Anchorage Alaska.
Orlic, B., Wassing, B.B.T., Geel, C.R., 2013. Field scale geomechanical modeling for prediction of fault stability during underground gas storage operations in a depleted gas field in the Netherlands. American Rock Mechanics Association, 47th U.S. Rock Mechanics/Geomechanics Symposium, ARMA 300, 11.
Pruess, K., Oldenburg, C., Moridis, G., 2011. TOUGH2 User's Guide, Version 2.1, LBNL-43134 (revised). Lawrence Berkeley National Laboratory, Berkeley, Calif.
Rutqvist, J., Wu, Y.-S., Tsang, C.-F., Bodvarsson, G., 2002. A modeling approach for analysis of coupled multiphase fluid flow, heat transfer, and deformation in fractured porous rock. Int. J. Rock Mech. Min. Sci. 39, 429–442.
Rutqvist, J., Dobson, P.F., Garcia, J., Hartline, C., Jeanne, P., Oldenburg, C.M., Vasco, D.W., Walters, M., 2015. The Northwest Geysers EGS demonstration project, California: pre-stimulation modeling and interpretation of the stimulation. Math. Geosci. 15, 48–66. http://dx.doi.org/10.1007/s11004-013-9493-y.
Rutqvist, J., 2011. Status of the TOUGH-FLAC simulator and recent applications related to coupled fluid flow and crustal deformations. Comput. Geosci. 37, 739–750.
Verdon, P.P., Kendall, J.M., White, D.J., Angus, D.A., 2011. Linking microseismic event observations with geomechanical models to minimize the risks of storing CO2 in geological formations. Earth Planet. Sci. Lett. 305, 143–152.
Willis-Richards, J., Watanabe, K., Takahashi, H., 1996. Progress toward a stochastic rock mechanics model of engineered geothermal systems. J. Geophys. Res. 101 (B8), 17481–17496.